Protective role of autophagy against *Vibrio cholerae* cytolysin, a pore-forming toxin from *V. cholerae*

Maximiliano Gabriel Gutierrez*, Hector Alex Saka†, Isabel Chinen‡, Felipe C. M. Zoppino*, Tamotsu Yoshimori§, Jose Luis Bocco†¶, and María Isabel Colombo*¶

*Laboratorio de Biología Celular y Molecular, Instituto de Histología y Embriología–Consejo Nacional de Investigaciones Científicas y Técnicas (CONICET), Facultad de Ciencias Médicas, Universidad Nacional de Cuyo, 5500 Mendoza, Argentina; †Departamento de Bioquímica Clínica, Centro de Investigaciones en Bioquímica Clínica e Inmunología–CONICET, Facultad de Ciencias Químicas, Universidad Nacional de Córdoba, 5000 Córdoba, Argentina; ‡Servicio de Fisiopatogenia, Instituto Nacional de Enfermedades Infecciosas, Administración Nacional de Laboratorios e Institutos de Salud ''Dr. Carlos G. Malbrán,'' 1281 Buenos Aires, Argentina; and §Department of Cell Genetics, National Institute of Genetics, Yata 1111 Mishima, Shizuoka 455-8540, Japan

Edited by Jeremy Nathans, The Johns Hopkins University School of Medicine, Baltimore, MD, and approved December 4, 2006 (received for review February 20, 2006)

Autophagy is the unique, regulated mechanism for the degradation of organelles. This intracellular process acts as a prosurvival pathway during cell starvation or stress and is also involved in cellular response against specific bacterial infections. *Vibrio cholerae* is a noninvasive intestinal pathogen that has been studied extensively as the causative agent of the human disease cholera. *V. cholerae* illness is produced primarily through the expression of a potent toxin (cholera toxin) within the human intestine. Besides cholera toxin, this bacterium secretes a hemolytic exotoxin termed *V. cholerae* cytolysin (VCC) that causes extensive vacuolation in epithelial cells. In this work, we explored the relationship between the vacuolation caused by VCC and the autophagic pathway. Treatment of cells with VCC increased the punctate distribution of LC3, a feature indicative of autophagosome formation. Moreover, VCC-induced vacuoles colocalized with LC3 in several cell lines, including human intestinal Caco-2 cells, indicating the interaction of the large vacuoles with autophagic vesicles. Electron microscopy analysis confirmed that the vacuoles caused by VCC presented hallmarks of autophagosomes. Additionally, biochemical evidence demonstrated the degradative nature of the VCC-generated vacuoles. Interestingly, autophagy inhibition resulted in decreased survival of Caco-2 cells upon VCC intoxication. Also, VCC failed to induce vacuolization in *Atg5*−/− cells, and the survival response of these cells against the toxin was dramatically impaired. These results demonstrate that autophagy acts as a cellular defense pathway against secreted bacterial toxins.

autophagosomes | LC3 | Rab7 | innate defense | cellular microbiology

Autophagy is an intracellular catabolic process that is activated in cells under conditions of stress, such as nutrient deprivation and growth factors (1, 2). It has been hypothesized that this degradative pathway evolved as a response to starvation and is the main component in the turnover of long-lived proteins in eukaryotic cells. In the last few years, this pathway has been associated with an increasing number of important functions (3–6). When autophagy is induced, isolation membranes sequester portions of cytosol, including organelles, and form a double-membrane structure called an "autophagosome" (7, 8). Autophagosomes mature by fusing with various endocytic compartments to ultimately degrade their content.

In recent years, the molecular machinery that regulates autophagy has begun to be revealed (9). In yeast, it has been shown that two ubiquitylation-like conjugation systems are required for autophagosome formation (10). The first conjugation system is the Atg5–Atg12 complex. The Atg5-Atg12 conjugate is essential for elongation of the isolation membrane (11). MAP-LC3 is a mammalian homologue of Atg8 in yeast and is part of the second conjugation system that leads to the covalent linkage between LC3 and phosphatidylethanolamine (12). It has been shown that LC3 exists in two forms: the cytosolic form (LC3-I) and the processed form (LC3-II) located on the autophagosomal membrane. LC3 processing is activated when autophagy is induced (12).

Vibrio cholerae is a noninvasive pathogen that produces cholera, a disease characterized by profuse watery diarrhea, which is potentially highly lethal and occurs as epidemics or even pandemics that mainly affect developing countries (13, 14). A potent enterotoxin, termed cholera toxin (CT), and a colonization factor, termed toxin coregulated pilus (TCP), are critically involved in the pathogenesis of cholera (14, 15). Besides CT and TCP, *V. cholerae* generates several additional secreted proteins that possess well characterized cytotoxic activity *in vitro* (16, 17). *V. cholerae* cytolysin (VCC) is an exotoxin produced by most O1 biotype El Tor and non-O1/non-O139 *V. cholerae* isolates (18, 19) encoded by the *hlyA* gene (20). This cytotoxic factor is a pore-forming toxin that causes vacuolization or cell lysis and necrosis, depending on the cell type and toxin concentration (21–25). It has been proposed that VCC contributes to the pathogenesis of gastroenteritis, particularly in strains that do not produce CT (26). A potent cell-vacuolating activity of VCC has been described (23, 25), but the membrane traffic processes involved in vacuole biogenesis are still poorly understood, although late endosomes, autophagosomes, and the Golgi complex may contribute to vacuole formation (25, 27).

Recently, the role of the autophagic pathway in protecting mammalian cells against various human bacterial pathogens has been demonstrated (28–31). However, the role of autophagy in response to bacterial toxins is still unknown. In this study, we present evidence that a secreted toxin from *V. cholerae* (VCC) is able to modulate autophagy in target cells. We also show that this autophagic response is necessary to override the cytotoxic effect of VCC and prevent cell death.

Results

VCC Is a Secreted Toxin of *V. cholerae* That Causes Autophagy. To study the relationship between VCC intoxication and autophagy, CHO cells stably overexpressing GFP-LC3 (CHO-LC3) (32) were exposed to sterile culture supernatants obtained from a CT-negative *V. cholerae* strain or from its isogenic *hlyA* null mutant

Author contributions: M.G.G. and H.A.S. contributed equally to this work; M.G.G., H.A.S., J.L.B., and M.I.C. designed research; M.G.G., H.A.S., and F.C.M.Z. performed research; I.C., F.C.M.Z., and T.Y. contributed new reagents/analytic tools; M.G.G., H.A.S., J.L.B., and M.I.C. analyzed data; and M.G.G. wrote the paper.

The authors declare no conflict of interest.

This article is a PNAS direct submission.

Abbreviations: BHI, brain–heart infusion broth; CT, cholera toxin; MEF, mouse embryonic fibroblasts; NEM, *N*-ethylmaleimide; 3-MA, 3-methyladenine; VCC, *Vibrio cholerae* cytolysin.

¶To whom correspondence may be addressed. E-mail: jbocco@fcq.unc.edu.ar or mcolombo@fcm.uncu.edu.ar.

This article contains supporting information online at www.pnas.org/cgi/content/full/0601437104/DC1.

© 2007 by The National Academy of Sciences of the USA

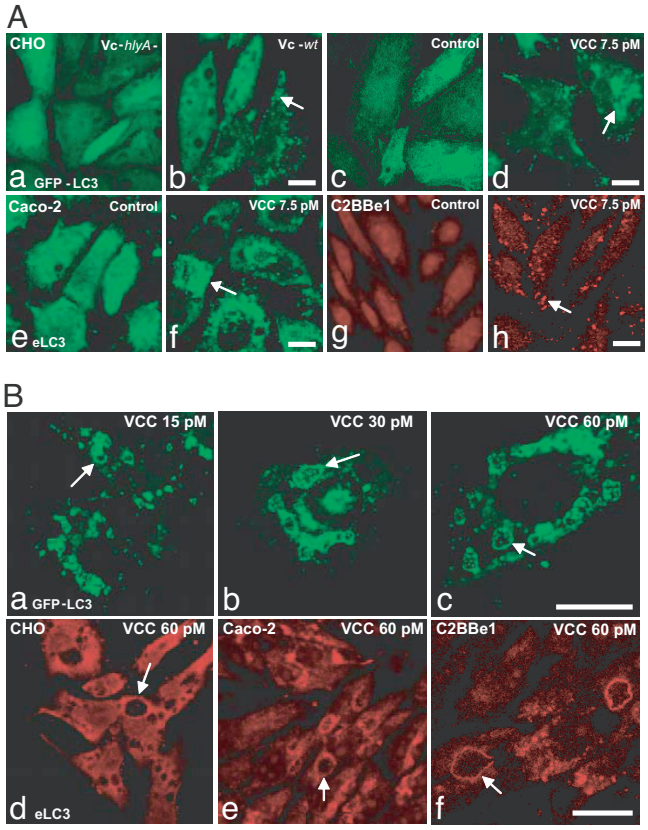

Fig. 1. Autophagy induction in cells intoxicated with VCC. (*A*) VCC is a secreted hemolysin from *V. cholerae* that causes autophagy in several cell lines. (*Aa–Ad*) CHO-LC3 cells were incubated for 4 h with a filter-sterilized supernatant from *V. cholerae wt* (Vc-*wt*) (*Ab*) or *hlyA*$^-$ (Vc-*hlyA*$^-$) (*Aa*) diluted 1:100. *Ac* and *Ad* show CHO-LC3 with or without the addition of 7.5 pM purified VCC for 4 h. (*Ae–Ah*) Detection by indirect immunofluorescence of endogenous LC3 in human colonic-derived Caco-2 cells (*Ae* and *Af*) and in C2BBe1 cells (brush border-expressing Caco-2 clone) (*Ag* and *Ah*) with or without the addition of 7.5 pM VCC for 4 h. Arrows indicate punctate LC3-labeled structures. Confocal images are depicted. (Scale bars: 10 μm.) (*B*) LC3 colocalizes with the VCC-generated vacuoles. (*Ba–Bc*) CHO-LC3 cells were treated with different concentrations of VCC as indicated (15–60 pM) for 4 h. Increasing concentrations of the toxin induce not only a clear targeting of GFP-LC3 to punctate structures but also localization of GFP-LC3 to the limiting membrane of the VCC-generated vacuoles, as well as to the small internal vesicles. (*Bd–Bf*) Cells were intoxicated with VCC 60 pM as described above and subjected to immunofluorescence to detect endogenous LC3 in CHO, Caco-2, and C2BBe1 cells. Arrows indicate vacuoles decorated by LC3. Confocal images are depicted. (Scale bars: 10 μm.)

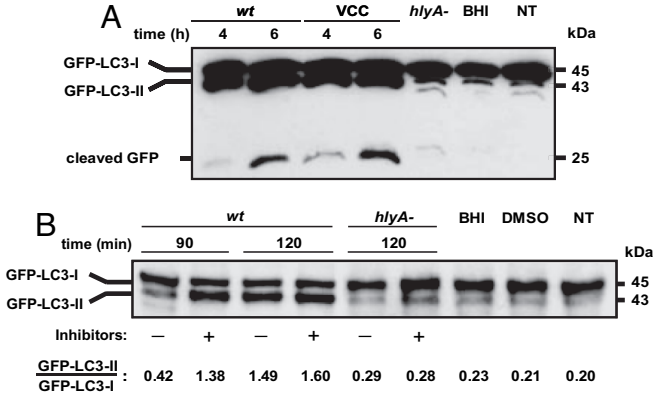

Fig. 2. LC3 processing upon VCC intoxication. (*A*) VCC enhances LC3 processing. CHO-LC3 cells were incubated with filter-sterilized culture supernatants from Vc-*wt* or Vc-*hlyA*$^-$ (1:100 dilution), with purified VCC (60 pM), or with noninoculated BHI medium (1:100 dilution). After the indicated incubation times, protein cell extracts were subjected to SDS/PAGE and the GFP-LC3 forms (I and II) or free cleaved GFP were detected by Western blot analysis, as described in *Materials and Methods*. NT, nontreated. (*B*) Inhibition of lysosomal proteases leads to LC3-II accumulation during VCC-induced autophagy. Shown is a representative immunoblot of CHO-LC3 cells treated with sterile culture supernatants from Vc-*wt* or Vc-*hlyA*$^-$ (1:100 dilution), with or without previous incubation with pepstatine A (10 μg/ml) and E64d (10 μg/ml) 2 h before stimuli. As control, cells treated only with 1:100 dilution of BHI, 0.1% vol/vol DMSO (120 min each), and NT cells were assayed. Protein extracts were obtained and analyzed by Western blotting using an anti-GFP antibody.

defective in VCC [see *Material and Methods* and supporting information (SI) Fig. 6]. As shown in Fig. 1*Ab*, a 1:100 dilution of a sterile culture supernatant from the *V. cholerae* wild-type strain clearly induced GFP-LC3 targeting to punctated structures. When CHO-LC3 cells were incubated with the same dilution of sterile culture supernatant from the *V. cholerae hlyA* null mutant strain, no changes in GFP-LC3 distribution were observed (Fig. 1*Aa*). To confirm that the effects observed with supernatants were indeed caused by the toxin, purified VCC was used. As expected, purified VCC induced GFP-LC3 punctate distribution (Fig. 1*Ad*), whereas no changes in GFP-LC3 distribution were induced under control conditions (Fig. 1*Ac*) or after the addition of heat-inactivated VCC (SI Fig. 7). In agreement with these observations, we also noted an intense redistribution of the endogenous LC3 in CHO and HEK cells (data not shown).

As mentioned above, the LC3 protein is processed for lipid conjugation upon autophagy induction, leading to a downward shift in its electrophoretic mobility. As shown in Fig. 2*A*, incubation of CHO-LC3 cells with VCC markedly enhanced the concentration of the lipidated LC3 form (known as "LC3-II" or "processed LC3"). It has been shown that the LC3-II trapped inside autophagosomes is degraded by lysosomal hydrolases after the formation of autolysosomes, and the lysosomal turnover of LC3-II, not a transient increase, is indicative of autophagy induction (33). To determine whether VCC is inducing autophagy and not blocking this pathway with a consequent increase in the LC3-II form, an experiment using inhibitors of lysosomal enzymes was performed. When cells treated with Vc-*wt* supernatant were preincubated with lysosomal protease inhibitors, the amount of GFP-LC3-II was increased substantially after 90 min of treatment, compared with cells treated with Vc-*wt* supernatant alone (Fig. 2*B*). This result indicates that VCC is actually inducing autophagy and not impairing this process. Moreover, experiments using DQ BSA, a fluorophore dequenching upon proteolysis and colocalization with Cathepsin D, further supported the degradative nature of VCC-generated vacuoles (SI Fig. 8). In addition, it has been shown that the GFP fragment is relatively stable to proteolysis and therefore accumulates in an autophagy-dependent manner both in yeast and in mammalian cells (6, 34). As shown in Fig. 2*A*, the increased levels of free cleaved GFP correlated well with LC3 conversion. Therefore, the accumulation of free cleaved GFP provides additional support regarding the normal progression of the autophagic pathway in VCC-treated cells.

Taken together these results clearly indicate that VCC is the component of *V. cholerae* supernatant capable of triggering autophagy.

Because epithelial intestinal cells are the main target of VCC *in vivo*, we studied the intracellular distribution of LC3 in related cell lines after treatment with VCC. As observed for CHO cells in the human colonic-derived Caco-2 and C2BBe1 cells, under control conditions, endogenous LC3 showed a cytosolic pattern with a low level of LC3 redistribution. However, incubation with a low dose of VCC resulted in a remarkable increase in the punctate distribution of LC3 (Fig. 1 *Af* and *Ah*). This redistribution was also observed in

Caco-2 and C2BBe1 cells after treatment with supernatants from *V. cholerae* wild type but not with the *V. cholerae hlyA* null mutant (data not shown). Taken together, these results indicate that VCC is a secreted toxin of *V. cholerae* that causes autophagy induction in different cells, including human colonic cell lines.

LC3 Colocalizes with VCC-Generated Vacuoles in a Broad Range of Toxin Concentrations. The above evidence prompted us to further investigate the contribution of the autophagic pathway to VCC-induced vacuoles. As mentioned previously, diverse cellular effects are observed, depending on toxin concentration (25, 27). Consequently, CHO-LC3 cells were exposed to several concentrations of purified VCC and we observed changes in GFP-LC3 distribution at all concentrations tested. However, the most remarkable finding was that the large VCC-generated vacuoles were clearly decorated with GFP-LC3 (Fig. 1 *Ba–Bc*). Given that LC3 is the best-characterized marker of autophagosomes to date, these data strongly suggest that autophagic compartments contribute to the generation of the vacuoles caused by VCC. A quantitative analysis indicated increased colocalization at higher toxin concentrations (data not shown). Interestingly, numerous vacuoles displaying characteristics of multivesicular bodies that contain internal GFP-LC3 vesicles were observed.

To further confirm our results, endogenous LC3 was detected by using a specific polyclonal antibody. As shown in Fig. 1*Bd*, endogenous LC3 localized in the VCC-generated vacuoles in CHO cells. Because different cell lines exhibit different sensitivity to VCC (27), we also detected the distribution of endogenous LC3 in Caco-2 and C2BBe1 (Fig. 1 *Be* and *Bf*), and the protein was strongly associated with the VCC-generated vacuoles in these cell types.

Ultrastructural Analysis of VCC-Generated Vacuoles. To corroborate that vacuoles caused by VCC presented autophagic characteristics, CHO cells were incubated with the toxin and subsequently analyzed by electron microscopy. As shown in Fig. 3*A*, VCC-generated vacuoles exhibited characteristics of autophagic vacuoles surrounded by double membranes (Fig. 3*Ab*, arrow), with multiple membranes inside and partially degraded intracellular material (Fig. 3 *Aa* and *Ac*). In line with confocal microscopy observations, the large vacuoles presented the typical multivesicular morphology, including several small vesicles within the large vacuoles (Fig. 3*A*). Moreover, the increased number of autophagosomes in the cytoplasm of the cells was in agreement with the vesicular pattern of LC3 described above. We next extended our analysis to Caco-2 cells. As shown in Fig. 3*Ad*, the vacuoles in these cells also exhibited autophagic characteristics. These results indicate that the VCC vacuoles are likely formed through interaction with autophagic compartments.

Autophagy Is Required for VCC-Dependent Vacuolization. Because the evidence presented here indicated that the autophagic pathway contributes to VCC-induced vacuolization, we tested the effect of autophagy inhibitors. CHO cells overexpressing GFP-LC3 were incubated with the toxin in the presence of the autophagy inhibitor 3-methyladenine (3-MA). As shown in Fig. 3*Bb*, this compound hampered not only LC3 redistribution but also the localization of GFP-LC3 to the generated vacuoles. Moreover, the number of vacuoles was markedly decreased, indicating that autophagy is essential for the biogenesis of the vacuoles (Fig. 3*B*, upper bar diagram).

The Atg5-dependent conversion of LC3 is a key step in autophagosome formation. We took advantage of Atg5-deficient mouse embryonic fibroblasts (*Atg5*−/− MEF) (35) to analyze the consequences in regard to VCC intoxication. As depicted in Fig. 3*Bc*, incubation of wild-type MEF cells with 60 pM VCC leads to an intense vacuolization clearly labeled by LC3. In contrast, *Atg5*−/− MEF cells were barely vacuolated, and LC3 remained cytosolic (Fig. 3*Bd*). A quantitative analysis indicates that in *Atg5*−/− MEF, the number of vacuoles was markedly reduced (Fig. 3*B*, lower bar diagram). Taken together, these results indicate that VCC-induced vacuolization is largely dependent on the autophagic pathway.

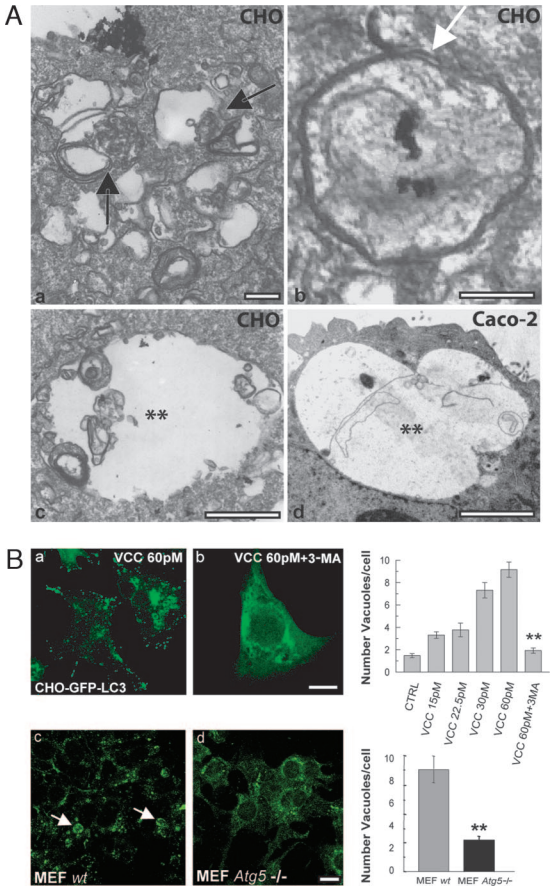

Fig. 3. VCC-induced vacuoles present hallmarks of autophagosomes. (*A*) VCC-generated vacuoles present characteristics of autophagosomal compartments. CHO cells (*Aa–Ac*) and Caco-2 cells (*Ad*) were incubated with 60 pM VCC for 4 h and processed for electron microscopy. Black arrows indicate vacuoles containing multiple membranes and partially degraded material. The white arrow indicates an autophagosome with double membranes. Asterisks indicate larger vacuoles with degraded material not surrounded by a double membrane, which likely represent mature autophagic vacuoles. (Scale bars: 1 μm.) (*B*) Autophagy is required for VCC-dependent vacuolization. CHO-LC3 cells were treated with 60 pM VCC or with 60 pM VCC plus 10 mM 3-MA for 4 h. In the presence of 3-MA, the number of vacuoles was markedly diminished and LC3 presented a cytosolic distribution (compare *Ba* and *Bb*). *Right* shows a quantitation of the number of vacuoles per cell at different VCC concentrations and the effect of 3-MA in cell vacuolation. MEF *wt* (*Bc*) and MEF *Atg5*−/− (*Bd*) were incubated with 60 pM VCC for 4 h. Cells were subjected to immunofluorescence to detect LC3. Arrows indicate generated vacuoles that colocalize with LC3. *Right* shows quantitation of the number of vacuoles per cell. (Scale bars: 10 μm.) Data are means ± SEM from at least three independent experiments. Fifty cells were counted in each experiment. **, significantly different from control ($P < 0.001$, ANOVA).

VCC Colocalizes to the Membranes of the GFP-LC3-Labeled Vacuoles Generated by the Toxin. It has been shown that, once VCC enters the cell, it associates with the membranes of vesicles (27). To determine whether the toxin was incorporated into the LC3-positive vacuoles generated by VCC, CHO-LC3 cells were incubated with the toxin, and VCC was detected by immunofluorescence. As shown in Fig. 4*A*, the toxin was clearly detectable in association with the vacuole membranes. This localization was particularly evident when vacuoles became larger. Remarkably, the toxin was also enclosed within

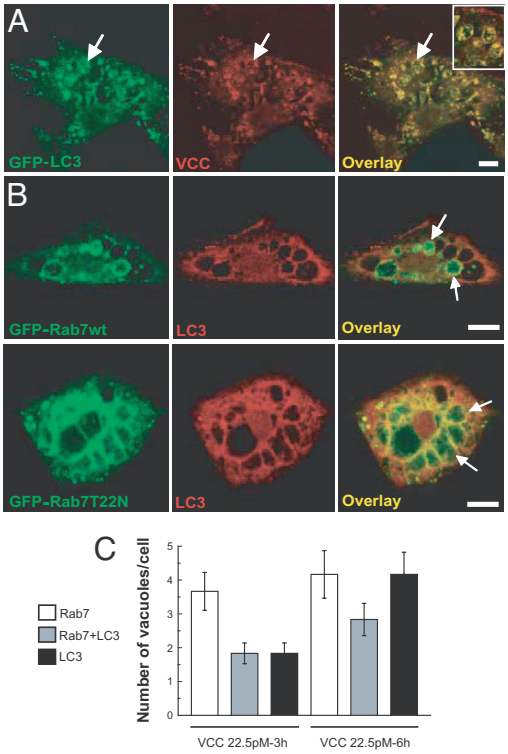

Fig. 4. Colocalization of VCC with LC3 and Rab7 on the toxin-generated vacuoles. (*A*) VCC is present on the LC3-labeled vacuoles. CHO-LC3 cells were incubated with 60 pM VCC for 4 h, and subsequently VCC was detected by immunofluorescence. Confocal images are depicted. Arrows indicate the large vacuoles with both GFP-LC3 and VCC localizing in the same vacuole. (*Inset*) A higher magnification of the image, depicting vacuoles with multivesicular body features. (*B*) Rab7-*wt* and Rab7-T22N decorate the LC3-labeled vacuoles generated by VCC. CHO cells overexpressing GFP-Rab7-*wt* (*Upper*) or GFP-Rab7-T22N (*Lower*) were treated with 60 pM VCC for 3 h, and endogenous LC3 was detected (red). Confocal images are depicted. Arrows indicate vacuoles positive for both markers. (Scale bars: 10 μm.) (*C*) Rab7-*wt* and LC3 colocalize with VCC-induced vacuoles. Bars represent the number of vacuoles per cell showing colocalization of LC3 and/or Rab7 with the VCC-generated vacuoles. At least 50 cells per condition were counted.

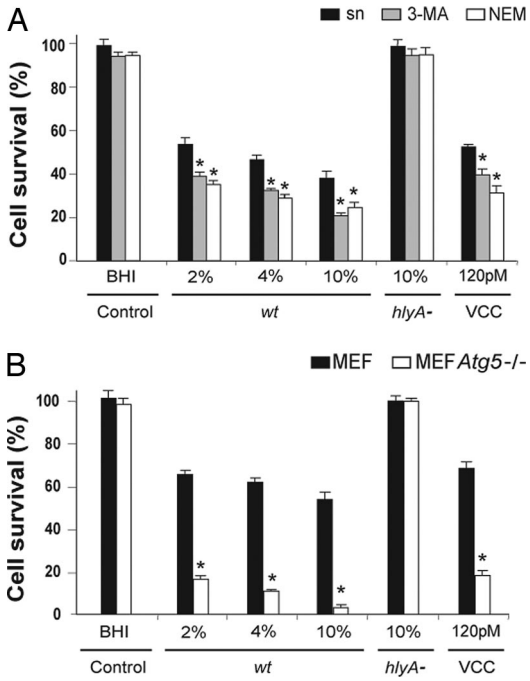

Fig. 5. Autophagy is required to improve cell survival upon VCC intoxication. (*A*) Autophagy inhibition increases cell death triggered by VCC. Caco-2 cells were incubated with increasing concentrations of filtered supernatants from Vc-*wt* or *hlyA*$^-$ or with purified VCC in the absence (black bars) or presence of 10 mM 3-MA (gray bars) or 20 μm NEM (white bars) to inhibit autophagy. After 4 h of treatment, cell viability was determined as described in *Material and Methods*. Control bars refer to cells incubated in the presence of 10% vol/vol BHI. Data represent the means ± standard deviation of at least three independent experiments. Asterisks indicate a statistically significant decrease in survival of cells treated with Vc-*wt* supernatant (sn) or with purified VCC in the presence vs. absence of 3-MA or NEM treatment ($P < 0.001$, Tukey–Kramer multiple comparisons test). (*B*) Atg5 is required for survival of cells intoxicated with VCC. MEF *wt* (black bars) and *Atg5*−/− MEF (white bars) cells were treated with Vc-*wt* or *hlyA*$^-$ supernatants (% vol/vol) or with 120 pM purified VCC, as indicated. After 4 h incubation, cell viability was determined as indicated above. Control bars refer to cells incubated in the presence of 10% vol/vol BHI. Data represented the means ± standard deviation of at least three individual experiments. Asterisks indicate a statistically significant decrease in survival of *Atg5*−/− MEF vs. MEF *wt* cells treated with Vc-*wt* supernatant or with purified VCC ($P < 0.001$, Tukey–Kramer multiple comparisons test).

the small vesicles labeled with LC3 that were contained inside the large LC3-positive vacuoles (Fig. 4*A Inset*).

Rab7 is a protein present on the membranes of autophagosomes that has been shown to be required for the normal progression of the autophagic pathway (36, 37). Thus, we next addressed whether the LC3-positive VCC-generated vacuoles were also positive for Rab7. For this purpose, CHO cells overexpressing GFP-Rab7-*wt* (36) were incubated with VCC, and the endogenous LC3 distribution was determined. As shown in Fig. 4*B*, upper panels, the majority of the vacuole membranes were labeled with the GFP signal. Indeed, we observed a mixed population of vacuoles, some labeled with both LC3 and Rab7, some with LC3 alone, and others with Rab7 alone (Fig. 4*C*). In cells overexpressing the GTPase-defective mutant of Rab7 (GFP-Rab7-Q67L), this protein also colocalized with LC3 on the membranes of the VCC-generated vacuoles (data not shown). Furthermore, in line with a previous report (27), we observed no inhibition of vacuolation when CHO cells overexpressing a dominant-negative mutant of Rab7 that does not bind GTP (GFP-Rab7-T22N) were incubated with the toxin. Additionally, the Rab7-negative mutant was associated with the membranes of the VCC-generated vacuoles (Fig. 4*B*, lower panels), as we described previously when autophagy was induced by amino acid deprivation (36).

Altogether, these results show that the toxin colocalized with LC3 on the vacuoles. In addition, Rab7, a GTPase associated with autophagic compartments, also colocalized with the VCC-generated vacuoles.

Cell Survival after Treatment with VCC: The Role of Autophagy. According to the evidence presented here, the vacuoles induced by VCC are related to the autophagic pathway. However, a relevant question was: What is the role of autophagy during this intoxication process? One of the direct cellular consequences of VCC is a potent cytocidal action (22). As expected, incubation of cells with several dilutions of the filtered supernatants obtained from *V. cholerae* wild-type strain caused a decrease in cell viability in a concentration-dependent manner (Fig. 5*A*). In contrast, incubation of cells with the *V. cholerae hlyA* null mutant culture supernatant did not affect cell survival.

On the basis of cumulative evidence indicating that autophagy plays a role in regulating cell survival vs. cell death, cells were treated with different inhibitors of autophagy. We previously showed that *N*-ethylmaleimide (NEM)-sensitive proteins seem to be required for the initial step of autophagosome formation (38). Upon VCC treatment, autophagy inhibition with 3-MA or NEM produced a mild decrease in cell survival (Fig. 5*A*). These data

suggest that autophagy increases the ability of cells to survive upon VCC intoxication. Furthermore, autophagy inhibition with 3-MA or NEM also decreased Caco-2 cell viability after incubation with purified VCC, thus confirming the results obtained with *V. cholerae* culture supernatants.

To further confirm the role of autophagy in cell survival, wild-type and *Atg5*−/− MEF cells were incubated with dilutions of the culture supernatants from both wild-type and *hlyA* null mutant *V. cholerae* strains. As shown in Fig. 5*B*, the lack of Atg5 dramatically decreased cell survival after treatment with *V. cholerae* wild-type culture supernatant or with purified VCC.

Taken together, these results indicate that autophagy is not only involved in cell vacuolation but also is required as a defensive response upon VCC intoxication.

Discussion

In the last few years, knowledge of the numerous mechanisms of action of bacterial toxins has increased enormously (39, 40). These studies have contributed both to molecular definition and to the discovery of important pathways in mammalian cells (41, 42). The autophagic pathway has been found to be involved in the elimination of certain intracellular pathogens (28–30); however, other microorganisms exploit autophagy to survive and replicate within specific intracellular compartments (43). In the present work, we used sterile culture supernatants from a CT-negative *V. cholerae* strain and from its isogenic *hlyA* null mutant, as well as purified VCC, and identified VCC as a *V. cholerae*-secreted toxin that triggers autophagy. Moreover, experimental evidence described here indicates that the autophagic process activated by VCC proceeds to completion. In this context, a clear enhancement of GFP-LC3-II accumulation was detected upon cell exposure to Vc-*wt* supernatant in the presence of lysosomal protease inhibitors (Fig. 2*B*). Additionally, the amount of cleaved free GFP increased progressively from 4 to 6 h after VCC intoxication. In agreement with this result, VCC-generated vacuoles display features of a degradative compartment, as measured by DQ BSA, and clearly colocalize with Cathepsin D, a lysosomal hydrolase.

Further experiments will be required in order to evaluate whether other toxins, absent from this *V. cholerae* strain, might also induce autophagy.

It has been proposed that VCC-induced vacuoles originate from various intracellular compartments (25, 27), suggesting that other intracellular pathways, beyond endocytosis, might contribute to the biogenesis of the vacuoles. The results given here clearly indicate that autophagy significantly contributes to the generation of the vacuoles. The observation of LC3-decorated membranes in VCC-generated vacuoles suggests that autophagic vesicles are compartments from which VCC-induced vacuoles likely derive. This intersection with autophagic compartments was confirmed at an ultrastructural level. Interestingly, we observed small internal vesicles positive for LC3 and VCC. The origin of these vesicles is likely explained by fusion of VCC vacuoles with double-membrane LC3-labeled vesicles. Another possibility is that the limiting membrane of the vacuoles could be internalized by microautophagy, a process that consists of direct invagination of membranes and subsequent budding of vesicles into the vacuolar lumen (44). Rab7 is a Rab protein present on autophagic structures that is also associated with the VCC-generated vacuoles (see ref. 27 and this article). However, overexpression of Rab7T22N did not block vacuolization (ref. 27 and this article). This observation is likely due to the fact that Rab7T22N impairs the final stages of autophagy but not autophagosome formation. Indeed, we have shown that this mutant causes autophagic vacuole accumulation (36).

Autophagy has been suggested to be an evolutionary conserved and self-limiting survival strategy (45). This pathway preserves cell viability in several systems, but it has been also linked to self-destruction (46). Results presented here with a bacterial toxin provide insights supporting the role of autophagy as a cell survival mechanism. Moreover, we present evidence that autophagy is a cellular response to a secreted pore-forming bacterial toxin such as VCC from *V. cholerae*. It is important to mention that the relationship between autophagy and toxins has been suggested before. Sandvig and van Deurs (47) reported that inhibitors of autophagy protect cells against ricin-induced lysis, suggesting that autophagy was required for cell lysis to occur. In contrast, we found that rather than being detrimental, the autophagic pathway is required in order to improve the survival of cells upon VCC intoxication. These differences could depend on the ability of each toxin to differentially modulate the autophagic pathway, thus determining the final outcome of cell viability. In the case of *Legionella*, a bacterial protein(s) is also able to induce autophagy, although the nature of the factor has not yet been identified (31).

An important observation is that autophagy induced by VCC is required for the survival of the cells, because when this pathway is inhibited cell death proceeds more rapidly. These observations are supported by two facts: (*i*) inhibition of autophagy with 3-MA, a well known inhibitor of autophagy, or with NEM, a compound also able to inhibit autophagosome formation (38), decreased cell survival; and (*ii*) cells unable to undergo autophagy, such as the *Atg5*−/− MEF, were highly sensitive to cell death upon VCC treatment. In a possible scenario, we suggest that epithelial cells respond to a low dose of the toxin with autophagy as a default protective pathway. Whether this phenomenon is a response of the cell itself, or is directly induced by the toxin, is yet to be determined. The response that causes massive vacuolization is likely related to the first attempt of the cells to survive. This hypothesis is in agreement with the observations that at low concentrations the toxin produces vacuolization, whereas higher concentrations lead to cell lysis (25, 27).

The discovery of a relationship between autophagy and cell damage induced by VCC is important for two main reasons. First, it aids in uncovering the exquisite molecular mechanisms that participate in the development of *V. cholerae* infection, and second, it is useful as a tool for investigating the role of autophagy as a cell survival response. In the context of bacterial pathogenesis, it is essential to determine whether autophagy is a protective intracellular pathway induced by other bacterial toxins as part of a more general mechanism.

Materials and Methods

Bacterial Strains, Supernatant Preparation, and VCC Purification. A non-O1/non-O139 *V. cholerae* strain (Vc-*wt*) isolated from a patient suffering from a cholera-like syndrome was used for this study. The strain was positive for the *hlyA* and *toxR* genes and negative for *ctxA*, *zot*, *ace*, *tcpA*, and *stn* genes, as determined by PCR analysis (48). An isogenic *hlyA* null mutant of this strain (Vc-*hlyA*$^-$) was obtained by insertional mutagenesis as described in ref. 49. Tn10-insertion into the *hlyA* gene was confirmed by PCR and DNA sequencing (SI Fig. 6). To obtain the sterile culture supernatants, Vc-*wt* and Vc-*hlyA*$^-$ were inoculated into brain–heart infusion broth (BHI) and incubated at 37°C for 16 h with shaking (120 rpm). These cultures were then centrifuged at 17,000 × *g* for 10 min at 4°C; the supernatants were sterilized through 0.22-μm low protein binding filters (Millipore, Billerica, MA) and kept on ice until use. Purified VCC was obtained as described in ref. 50.

Cell Culture. MEF, *Atg5*−/− MEF, and C2BBe1 cells were cultured by using DMEM supplemented with 10% vol/vol FBS, Caco-2 cells were cultured in DMEM supplemented with 20% FBS, and CHO cells were grown in MEM (α-MEM) supplemented with 10% FBS. Stably transfected CHO cells overexpressing GFP fusion proteins were supplemented with 0.2 mg/ml geneticin.

Indirect Immunofluorescence. Cells were grown on coverslips and incubated with purified VCC or with dilutions of the culture

supernatants from *V. cholerae*. Cells were fixed with 3% paraformaldehyde in PBS for 10 min at room temperature, washed with the buffer, and blocked with 50 mM NH_4Cl in PBS. Subsequently, cells were permeabilized with 0.05% saponin in PBS containing 0.2% BSA and then incubated with primary antibodies. A rabbit polyclonal anti-VCC (51) (dilution 1:50) or a mouse polyclonal affinity-purified anti-LC3 (dilution 1:50) were used. Antibodies against LC3 were raised in mice and purified by affinity chromatography from ascitic liquid. Bound antibodies were detected by incubation with Cy3- or Alexa 488-conjugated secondary antibodies (1:800 and 1:400, respectively) (Molecular Probes, Eugene, OR). Cells were mounted with Mowiol and examined by confocal fluorescence microscopy. Images were obtained with a Nikon C1 confocal microscope system and EZ-C1 software (Nikon, Tokyo, Japan). Images were processed by using Adobe 7.0 (Adobe Systems, San Jose, CA).

Transmission Electron Microscopy. Purified VCC was added to cells and, after 4 h of treatment, cells were fixed with 1% glutaraldehyde in 0.1 M cacodylate buffer (pH 7). Monolayers were scraped, postfixed in 2% osmium tetroxide in 100 mM cacodylate buffer, dehydrated with increasing concentrations of ethanol, and gradually infiltrated with Epon resin (Pelco, Redding, CA). Thin sections were stained with uranyl acetate and lead citrate and examined using a Zeiss (Thornwood, NY) EM 900 transmission electron microscope.

Quantification of Cell Viability. Cell viability was determined with the CellTiter aqueous nonradioactive cell proliferation assay (Promega, Madison, WI). This method allows the colorimetric determination of viable cells in cytotoxicity and also in proliferation assays. Its principle is based on detection of the bioreduction of the tetrazolium compound into a formazan product in the presence of an electron coupling reagent (phenazine methosulfate). Because this reaction is mediated by dehydrogenase enzymes found in metabolically active cells, the quantity of formazan produced is directly proportional to the number of living cells in culture. Cell viability assays were performed in accordance with the manufacturer's instructions (Technical Bulletin 169; Promega). Briefly, 2.5×10^4 cells were seeded into 96-well culture plates and incubated for 24 h. For autophagy blockade, cells were incubated with 10 mM 3-MA or 20 μM NEM for 1 h before the addition of sterile culture supernatants or purified VCC. After 4 h of treatment, absorbance at 490 nm was determined with a Bio-Rad (Hercules, CA) microplate reader.

Western Blot Analysis. Detection of forms I and II of the GFP-LC3 protein by Western blotting was performed essentially as described in ref. 12. Briefly, CHO-LC3 cells were cultured to ≈80% of confluence and treated with filter-sterilized culture supernatants from Vc-*wt* or Vc-*hlyA*$^-$ (1:100 dilution), with purified VCC (60 pM), with noninoculated BHI (1:100 dilution), or were left untreated. For inhibition of lysosomal protease enzymes, E64d and pepstatin A (Sigma-Aldrich, St. Louis, MO) (10 μg/ml each) were added to cell monolayers 2 h before treatment. After the indicated times, cells were washed in cold PBS, scraped, and lysed. For Western blot analysis, 50 μg of protein extracts were subjected to electrophoresis in 10% SDS/PAGE gels, transferred to a nitrocellulose membrane, and blocked with TBS 1× supplemented with 0.1% Tween 20/5% nonfat dry milk. The nitrocellulose membrane was incubated for 2 h with a rabbit polyclonal anti-GFP antibody (Abcam, Cambridge, MA) at a 1:2,000 dilution, washed, and incubated with a secondary HRP-conjugated anti-rabbit antibody (GE Healthcare, Bucks, U.K.) at a 1:10,000 dilution. After enhanced chemoluminescence reaction (SuperSignal West Pico system; Pierce, Rockford, IL), the bands were visualized upon exposition of nitrocellulose membrane to a ECL-hyperfilm (GE Healthcare).

We thank Dr. Noboru Mizushima (Tokyo Metropolitan Institute of Medical Science, Tokyo, Japan) for providing the *Atg*5−/− cells, Dr. Luis Mayorga for critical reading of this manuscript, Dr. Luis Patrito for continuous encouragement and support, and Marcelo Furlán and Alejandra Medero for technical assistance. This work was supported in part by Agencia Nacional de Promoción Científica y Tecnológica Grants PICT2002 no. 01-11004 (to M.I.C.) and PICT2003 no. 05-13446 (to J.L.B.) and by grants from Secretaría de Ciencia y Tecnología (Universidad Nacional de Cuyo and Universidad Juan Agustín Maza) (to M.I.C.) and from Secretaría de Ciencia y Tecnología (Universidad Nacional de Córdoba) (to J.L.B.). M.G.G., H.A.S., and F.C.M.Z. are CONICET Fellows. M.I.C. and J.L.B. are Career Investigator members of CONICET.

1. Klionsky DJ, Emr SD (2000) *Science* 290:1717–1721.
2. Reggiori F, Klionsky DJ (2005) *Curr Opin Cell Biol* 17:415–422.
3. Levine B, Yuan J (2005) *J Clin Invest* 115:2679–2688.
4. Levine B, Klionsky DJ (2004) *Dev Cell* 6:463–477.
5. Kuma A, Hatano M, Matsui M, Yamamoto A, Nakaya H, Yoshimori T, Ohsumi Y, Tokuhisa T, Mizushima N (2004) *Nature* 432:1032–1036.
6. Shintani T, Klionsky DJ (2004) *Science* 306:990–995.
7. Seglen PO, Berg TO, Blankson H, Fengsrud M, Holen I, Stromhaug PE (1996) *Adv Exp Med Biol* 389:103–111.
8. Mizushima N, Ohsumi Y, Yoshimori T (2002) *Cell Struct Funct* 27:421–429.
9. Reggiori F, Klionsky DJ (2005) *Curr Opin Cell Biol* 17:415–422.
10. Ohsumi Y (2001) *Nat Rev Mol Cell Biol* 2:211–216.
11. Mizushima N, Yamamoto A, Hatano M, Kobayashi Y, Kabeya Y, Suzuki K, Tokuhisa T, Ohsumi Y, Yoshimori T (2001) *J Cell Biol* 152:657–668.
12. Kabeya Y, Mizushima N, Ueno T, Yamamoto A, Kirisako T, Noda T, Kominami E, Ohsumi Y, Yoshimori T (2000) *EMBO J* 19:5720–5728.
13. Kaper JB, Morris JG, Jr, Levine MM (1995) *Clin Microbiol Rev* 8:48–86.
14. Faruque SM, Albert MJ, Mekalanos JJ (1998) *Microbiol Mol Biol Rev* 62:1301–1314.
15. Karaolis DK, Johnson JA, Bailey CC, Boedeker EC, Kaper JB, Reeves PR (1998) *Proc Natl Acad Sci USA* 95:3134–3139.
16. Fullner KJ, Boucher JC, Hanes MA, Haines GK, III, Meehan BM, Walchle C, Sansonetti PJ, Mekalanos JJ (2002) *J Exp Med* 195:1455–1462.
17. Silva TM, Schleupner MA, Tacket CO, Steiner TS, Kaper JB, Edelman R, Guerrant R (1996) *Infect Immun* 64:2362–2364.
18. Honda T, Finkelstein RA (1979) *Infect Immun* 26:1020–1027.
19. Yamamoto K, Al Omani M, Honda T, Takeda Y, Miwatani T (1984) *Infect Immun* 45:192–196.
20. Heidelberg JF, Eisen JA, Nelson WC, Clayton RA, Gwinn ML, Dodson RJ, Haft DH, Hickey EK, Peterson JD, Umayam L, *et al.* (2000) *Nature* 406:477–483.
21. Alm RA, Mayrhofer G, Kotlarski I, Manning PA (1991) *Vaccine* 9:588–594.
22. Zitzer A, Wassenaar TM, Walev I, Bhakdi S (1997) *Infect Immun* 65:1293–1298.
23. Coelho A, Andrade JR, Vicente AC, Dirita VJ (2000) *Infect Immun* 68:1700–1705.
24. Mitra R, Figueroa P, Mukhopadhyay AK, Shimada T, Takeda Y, Berg DE, Nair GB (2000) *Infect Immun* 68:1928–1933.
25. Figueroa-Arredondo P, Heuser JE, Akopyants NS, Morisaki JH, Giono-Cerezo S, Enriquez-Rincon F, Berg DE (2001) *Infect Immun* 69:1613–1624.
26. Pichel M, Rivas M, Chinen I, Martin F, Ibarra C, Binsztein N (2003) *J Clin Microbiol* 41:124–134.
27. Moschioni M, Tombola F, de Bernard M, Coelho A, Zitzer A, Zoratti M, Montecucco C (2002) *Cell Microbiol* 4:397–409.
28. Ogawa M, Yoshimori T, Suzuki T, Sagara H, Mizushima N, Sasakawa C (2005) *Science* 307:727–731.
29. Gutierrez MG, Master SS, Singh SB, Taylor GA, Colombo MI, Deretic V (2004) *Cell* 119:753–766.
30. Nakagawa I, Amano A, Mizushima N, Yamamoto A, Yamaguchi H, Kamimoto T, Nara A, Funao J, Nakata M, Tsuda K, *et al.* (2004) *Science* 306:1037–1040.
31. Amer AO, Swanson MS (2005) *Cell Microbiol* 7:765–778.
32. Gutierrez MG, Vazquez CL, Munafo DB, Zoppino FC, Beron W, Rabinovitch M, Colombo MI (2005) *Cell Microbiol* 7:981–993.
33. Tanida I, Minematsu-Ikeguchi N, Ueno T, Kominami E (2005) *Autophagy* 1:84–91.
34. Hosokawa N, Hara Y, Mizushima N (2006) *FEBS Lett* 580:2623–2629.
35. Mizushima N, Yamamoto A, Hatano M, Kobayashi Y, Kabeya Y, Suzuki K, Tokuhisa T, Ohsumi Y, Yoshimori T (2001) *J Cell Biol* 152:657–668.
36. Gutierrez MG, Munafo DB, Beron W, Colombo MI (2004) *J Cell Sci* 117:2687–2697.
37. Jager S, Bucci C, Tanida I, Ueno T, Kominami E, Saftig P, Eskelinen EL (2004) *J Cell Sci* 117:4837–4848.
38. Munafo DB, Colombo MI (2001) *J Cell Sci* 114:3619–3629.
39. Schiavo G, van der Goot FG (2001) *Nat Rev Mol Cell Biol* 2:530–537.
40. Sandvig K, Spilsberg B, Lauvrak SU, Torgersen ML, Iversen TG, van Deurs B (2004) *Int J Med Microbiol* 293:483–490.
41. Sandvig K, van Deurs B (2002) *FEBS Lett* 529:49–53.
42. Sandvig K, van Deurs B (2002) *Annu Rev Cell Dev Biol* 18:1–24.
43. Kirkegaard K, Taylor MP, Jackson WT (2004) *Nat Rev Microbiol* 2:301–314.
44. Kunz JB, Schwarz H, Mayer A (2004) *J Biol Chem* 279:9987–9996.
45. Lum JJ, Bauer DE, Kong M, Harris MH, Li C, Lindsten T, Thompson CB (2005) *Cell* 120:237–248.
46. Levine B, Yuan J (2005) *J Clin Invest* 115:2679–2688.
47. Sandvig K, van Deurs B (1992) *Exp Cell Res* 200:253–262.
48. Bidinost C, Saka HA, Aliendro O, Sola C, Panzetta-Duttari G, Carranza P, Echenique J, Patrito E, Bocco JL (2004) *Rev Argent Microbiol* 36:158–163.
49. Herrero M, de Lorenzo V, Timmis KN (1990) *J Bacteriol* 172:6557–6567.
50. Yamamoto K, Al Omani M, Honda T, Takeda Y, Miwatani T (1984) *Infect Immun* 45:192–196.
51. Chinen I, Toma C, Honma Y, Higa N, Iwanaga M (1996) *Jpn J Trop Med Hyg* 24:151–155.